Available online at www.sciencedirect.com

SciVerse ScienceDirect

Ceramics International 39 (2013) 771–777

CERAMICS INTERNATIONAL

www.elsevier.com/locate/ceramint

Synthesis of nanoscale hydroxyapatite particles using triton X-100 as an organic modifier

E. Iyyappan, P. Wilson*

Madras Christian College, Department of Chemistry, East Tambaram, Chennai 600 059, Tamil Nadu, India

Received 28 February 2012; received in revised form 21 June 2012; accepted 29 June 2012
Available online 6 July 2012

Abstract

Nano-sized rod like hydroxyapatite (HA) particles were synthesized using $Ca(NO_3)_2 \cdot 4H_2O$ and $(NH_4)_2HPO_4$ as precursors with varying contents of non-ionic surfactant viz., p-(1,1,3,3-tetramethylbutyl)phenoxypoly(oxyethylene)glycol (triton X-100) as organic modifer. The crystalline phase, chemical composition, surface area and morphology of the prepared samples were characterized by X-ray diffraction (XRD), Fourier transform infrared spectroscopy (FTIR), BET surface area analysis, high resolution scanning electron microscopy (HRSEM) and transmission electron microscopy (TEM). The above studies indicate the presence of nanoscale hydroxyapatite (HA) phase. Triton X-100 does not appear to affect the crystallinity of the samples. Increase of BET surface area and the consequent decrease in particle size of HA were observed as a function of surfactant content. Probable mechanism for the role of the surfactant in the synthesis of nanoscale HA has also been discussed.

Keywords: Triton X-100; Non-ionic surfactant; Nanoscale hydroxyapatite

1. Introduction

Synthetic hydroxyapatite [$(Ca_{10}(PO_4)_6(OH)_2$] resembles the mineral component of bone and tooth, hence possesses enormous biocompatibility and bioactivity. However densified HA, fabricated with HA powders of large particle size, has low tensile strength and fracture toughness on comparison with natural bone, thus restricting their use to less stressful applications [1]. However, a fine layer of synthetic HA coating on mechanically reliable implants has been made to increase their biocompatibility and bioactivity [2]. It is reasonable to expect that the nanoscale HA particles would serve as a promising material for orthopedic and dental implant applications owing to its enhanced bioactivity with improved osseointegrative properties. Moreover natural bone consists of HA nanorods embedded in collagen matrix. Thus synthesis and fabrication of HA nanorod based materials are beneficial when one considers the biocompatibility of the synthesized HA. In addition, HA and its substituted versions have also been investigated for their catalytic activity for many organic transformations [3–5]. Besides, hydroxyapatite materials have also been established to be effective adsorbents for amine fluorides, citric acid, certain proteins and heavy metal ions [6–9]. Further, HA powders are used as delivery agents for antibiotics, proteins and anticancer drugs [10–12]. Thus it is readily comprehensible that nanoHA with higher surface area and lower particle size can provide higher biocompatibility, greater catalytic activity and good adsorption capability for use as biomaterial, catalyst and adsorbent respectively.

There are various methods to synthesize nano-sized hydroxyapatite crystals; they are namely mechano-chemical method [13], sol–gel route [14], chemical precipitation [15], hydrothermal method [16], microemulsion method [17], ultrasonic irradiation [18], microwave irradiation [19] and surfactant assisted routes [20]. Among various preparative methods, chemical precipitation in aqueous media is found to be superior in synthesizing HA with high phase purity and desired morphology even at low temperatures [21]. On the other hand, surfactant assisted method has been proved to be a promising technique to synthesize hydroxyapatite particles of nano dimensions [22].

*Correspondence to: F2, Elim Homes, No. 9, Bethelpuram, East Tambaram, Chennai-600 059, India. Tel.: +91 44-9841426693.
E-mail address: catwils@gmail.com (P. Wilson).

0272-8842/$36.00 © 2012 Elsevier Ltd and Techna Group S.r.l. All rights reserved.
http://dx.doi.org/10.1016/j.ceramint.2012.06.090

Recently, Chaofan Qiu et al. have prepared nano-sized HA by using polyethylene glycol (PEG) as organic modifier. Their study indicates that PEG could efficiently hinder the nucleation and growth of HA through the interaction of functional group –CH_2–CH_2–O– with Ca^{2+} ions in the HA precursor. It has also been proved that HA with lower particle size and poor crystallinity has resulted when high concentrations of PEG were used [23]. Incidentally, it can be inferred that both PEG and triton X-100 possess similar functional group –CH_2–CH_2–O– as a part of their structure. This provoked us to reflect on employing the non ionic surfactant viz., triton X-100 as organic modifier in place of PEG to synthesize HA with better morphological and pore characteristics along with particles of nanorange. In addition, Jingxian Zhang et al., have synthesized triton X-100/HA nanocomposites with rod like morphology by using triton X-100 as a template and they have also demonstrated the decrease of grain size with increasing triton X-100 content through XRD studies [24].

2. Experimental

2.1. Materials and methods

The chemicals used in the present investigation were Ca $(NO_3)_2.4H_2O$ (sd fine-Chem. Ltd.), $(NH_4)_2HPO_4$ (Merck Specialities Pvt. Ltd.), liquor ammonia (Qualigens fine chemicals) and triton X-100 with composition $C_{14}H_{22}O$ $(C_2H_4O)_n$ (n=9–10) (Sisco Research Laboratories Pvt. Ltd.). All chemicals were of analytical grade and used without further purification.

2.1.1. The specific conductivity measurements

Specific conductivities were measured for calcium nitrate solutions (0.4 M) with varying amounts of triton X-100 using conductivity meter (DIGISUN make) in order to investigate the possibility of interaction if any with triton X-100 during the nucleation and growth of HA.

2.1.2. Synthesis of hydroxyapatite

100 mL of 0.24 M diammonium hydrogen phosphate solution (pH 10.4; adjusted using 1:1 NH_3) was taken in a 500 mL beaker and 100 mL of 0.4 M solution of $Ca(NO_3)_2$ (pH 10.4; adjusted using 1:1 NH_3) was added drop wise from a burette while stirring the content of the beaker using magnetic stirrer. Adequate care was taken to maintain pH of the reaction mixture above 10 through proper addition of 1:1 NH_3 besides the addition of $Ca(NO_3)_2$ solution. A milky suspension formed was refluxed for an hour, cooled and centrifuged. The white precipitate thus obtained was dried over night in hot air oven at 120 °C and a portion of it was calcined at 600 °C for 2 h in stagnant air. The samples prepared through chemical precipitation will hereafter be designated as HA-CP. The above procedure was repeated with calcium nitrate solution containing varying content of triton X-100 namely (2%, 4%, and 6% (w/v)). The samples prepared through surfactant-assisted route will hereafter be designated as HA-SA. Flow chart for the synthesis of HA-CP and HA-SAs is depicted in Fig. 1.

2.2. Characterization

2.2.1. X-ray diffraction (XRD)

X-ray diffractograms were recorded for the fresh and calcined HA samples prepared by chemical precipitation and surfactant assisted route using Guiner powder diffractometer (SAIFERT BYZ 2002 MODEL) between 2θ values of 20 and 70 using CuKα as source. The d values corresponding to the first five intense peaks were calculated and compared with the ASTM files for the identification of HA phase.

2.2.2. Fourier transform infrared spectroscopy (FTIR)

FTIR spectra were recorded for the fresh and calcined samples of HA-CP and HA-SAs between 450 and 4000 cm^{-1} using an IR-OPUS SOFTWARE FTIR model spectrophotometer by KBr pellet technique.

2.2.3. BET surface area measurements

BET surface area measurements were carried out with MICROMERITICS ASAP 2020 V3.00H for calcined samples of HA-CP and HA-SAs.

2.2.4. High resolution scanning electron microscopic analysis (HRSEM)

High resolution SEM images were recorded using QUANTA-200 scanning electron microscope for selected calcined samples viz., HA-CP and HA-SA (4% triton X-100).

2.2.5. Transmission electron microscopy (TEM)

TEM analysis was performed for selected samples using a HITACHI H-7650 Transmission Electron Microscope with an accelerating voltage of 80 kV. Sampling was accomplished by dispersing small amount of HA powder in ethanol by sonicating for 20 min, with the subsequent addition of a drop of suspension on the carbon coated copper mesh followed by drying in air.

3. Results and discussion

3.1. Conductivity measurements

Table 1 lists the specific conductivities of $Ca(NO_3)_2$ solution with varying amount of triton X-100. Specific conductivity was found to decrease with increasing amount of triton X-100 suggesting the existence of possible interaction between triton X-100 and Ca^{2+} ions in solution. This interaction between triton X-100 and Ca^{2+} ions is bound to influence the nucleation and growth of HA [23]. The expectation that the interaction mentioned above might result in affecting the morphology and particle size of HA, led the present investigation to use triton X-100 as organic modifier for the synthesis of HA.

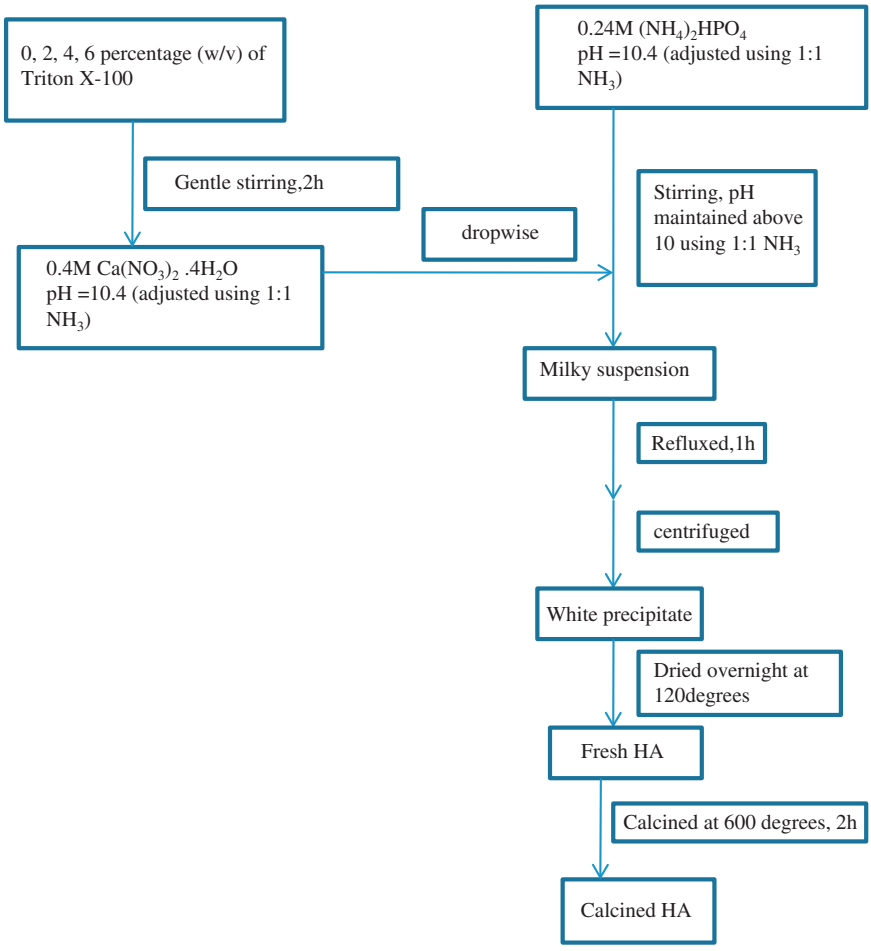

Fig. 1. Flow chart for the synthesis of HA-CP and HA-SAs.

Table 1
Specific conductivities of $Ca(NO_3)_2$ solution as a function of Triton X-100 content.

Sl. no.	% by wt of Triton X-100	Specific conductivity ($\times 10^{-3}$ S cm^{-1})
1	0	44.3
2	2	43.7
3	4	41.9
4	6	39.7

3.2. X-ray diffraction studies

The XRD patterns of fresh and calcined samples of HA-CP and HA-SAs are shown in Figs. 2 and 3 respectively. The peaks corresponding to all HA samples found at $2\theta = 25.5$, 31.6, 32.6, 46.3 and 49.09 were found to match well with the standard data (JCPDS card no. 09-432) indicating the presence of HA phase. It is interesting to note that there are no other phases such as tricalcium phosphate present in the sample even on calcination. This further highlights the advantage of this method. All the fresh samples viz., HA-CP and HA-SA were found to have good crystallinity as evidenced by the presence of sharp XRD peaks. This result appears to be contrary to the report found elsewhere [23], where employing polyethyleneglycol (PEG) as organic modifier yielded HA samples of poor crystallinity particularly when high concentration of organic modifier was used.

3.3. Fourier transform infrared spectral studies

The FTIR spectra of fresh samples of HA-CP and HA-SAs are shown in Fig. 4 and that of calcined samples are shown in Fig. 5. FTIR spectral pattern indicates that both fresh and calcined samples of HA-CP and HA-SAs correspond to HA. The bands at 3572 and 633 cm^{-1} are characteristic of structural OH of HA. The stretching vibrational modes of PO_4^{3-} group appears at 1093, 1036 and 962 cm^{-1}, while the bands at 602, 565 and 472 cm^{-1} correspond to the O–P–O bending modes. In addition, the broad band centered at approximately 3400 cm^{-1} and that at 1624 cm^{-1} show the presence of adsorbed water, essentially present in fresh samples. However, the bands corresponding to 1479, 1422 and 876 cm^{-1} imply the presence of carbonate ion in the resultant HA, while the XRD pattern validates the presence of pure HA. These facts together insinuate that the bands corresponding to carbonate are due to the physical interaction of HA with carbon dioxide during synthesis, under ambient conditions.

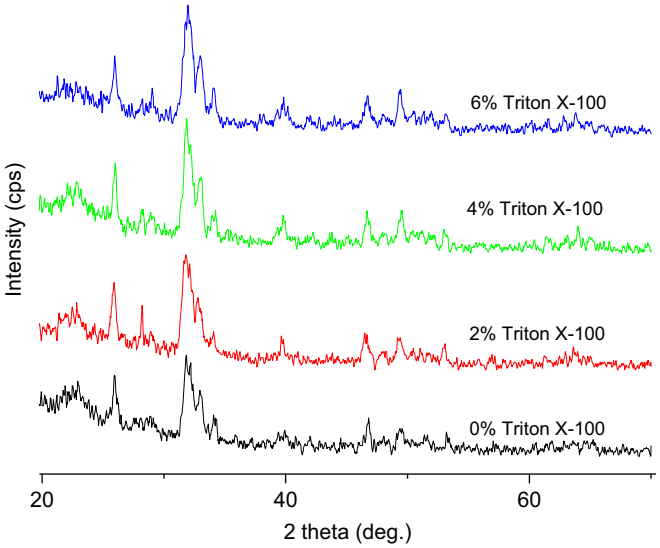

Fig. 2. XRD patterns of fresh samples of HA-CP and HA-SAs.

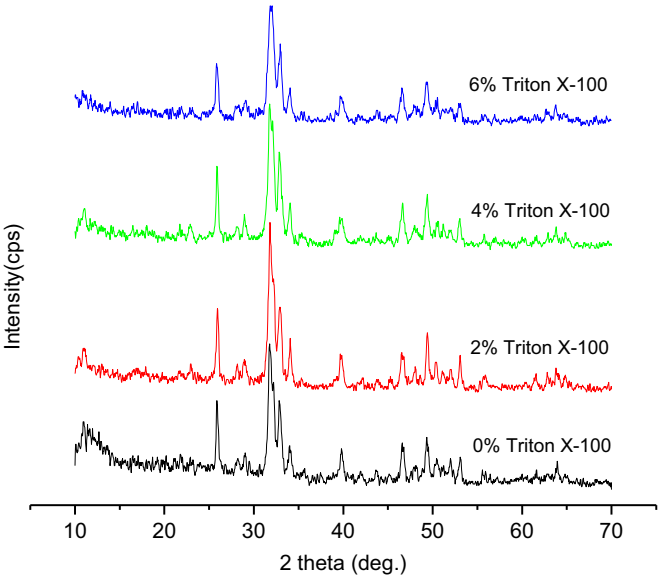

Fig. 3. XRD patterns of calcined samples of HA-CP and HA-SAs.

The bands characteristic of C–H stretch of CH_3 and CH_2 groups viz., 2928 and 2856 cm^{-1} respectively were found to be absent in FTIR spectra corresponding to all the fresh and calcined samples. This confirms the complete removal of triton X-100 from the prepared samples under given preparation conditions. On calcination, the bands due to structural hydroxyl group and phosphate group become highly pronounced owing to the enhanced crystallinity.

3.4. BET surface area analysis

BET surface area of calcined HAs was measured for all the samples and the equivalent particle sizes were calculated (theoretically) using the formula $d=6/\rho A$ where d, ρ and A are particle size, theoretical density (3.156 g/cm^3) and specific surface area respectively of the HA particles as

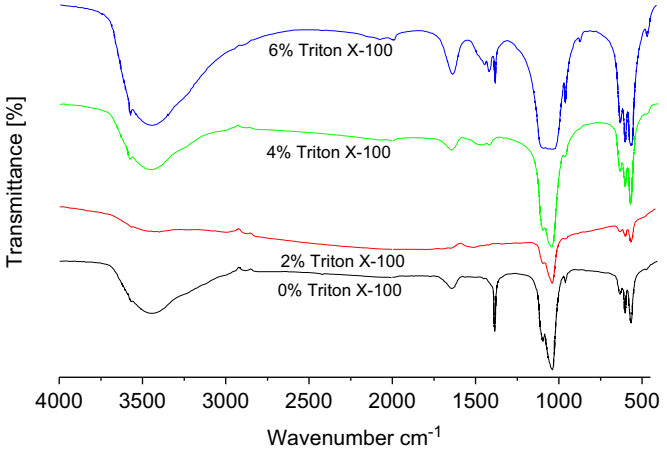

Fig. 4. FT-IR spectra of fresh samples of HA-CP and HA-SAs.

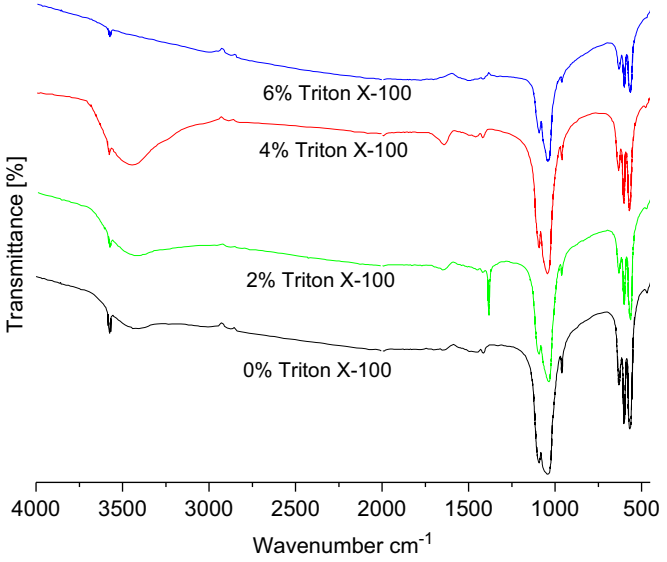

Fig. 5. FT-IR spectra of calcined samples of HA-CP and HA-SAs.

referred elsewhere [25]. BET surface and equivalent particle size of HA-CP and HA-SAs are listed in Table 2.

BET surface area of calcined samples of HA-SAs is found to be larger than calcined sample of HA-CP. In addition, BET surface area is found to increase with the increase in surfactant content. As expected the particle size of calcined samples of HA-SA is smaller than that of calcined samples of HA-CP.

3.5. Scanning electron microscopic analysis

Figs. 6 and 7 show the high resolution SEM micrographs of calcined samples of HA-CP and HA-SA (4% triton X-100) respectively. It is evident from the comparison of high resolution micrographs that HAs prepared by surfactant assisted route are composed of relatively smaller sized particles than that prepared by chemical precipitation method. Comparing the enhanced BET surface area of the samples prepared through surfactant assisted route with

Table 2
BET surface and equivalent particle size of HA-CP and HA-SAs.

Calcined HA	Surface area (m^2/g)	Equivalent particle size (nm)
HA-CP	37.8	50
HA-SA (2% Triton X-100)	40.8	47
HA-SA (4% Triton X-100)	44.5	43
HA-SA (6% Triton X-100)	51.5	37

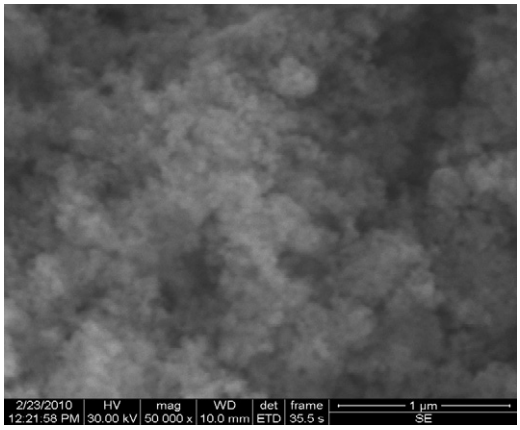

Fig. 6. HRSEM micrograph of calcined HA-CP (0% Triton X-100).

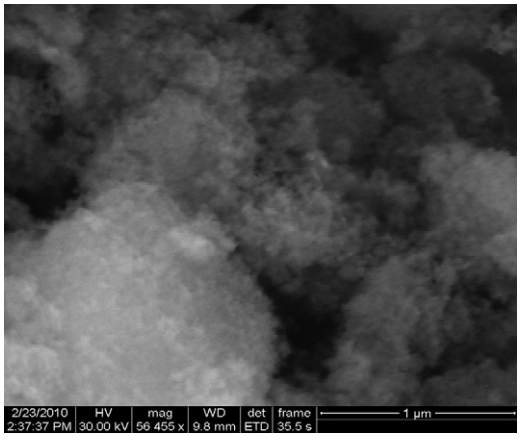

Fig. 7. HRSEM micrograph of calcined HA-SA (4% Triton X-100).

that of chemical precipitation, one could comprehend that the hampering of agglomeration and reduction in particle size, as evident from SEM micrographs, contribute to a large extent for the increased surface area of samples synthesized by the use of triton X-100. However shape of the HA particles are not clearly defined in the SEM images obtained in the present investigation.

3.6. Transmission electron microscopic analysis

Figs. 8 and 9 show the TEM images of calcined samples of HA-CP and HA-SA (4% triton X-100) respectively. From Fig. 8 it is evident that the HA-CP sample prepared without triton X-100 shows the presence of highly

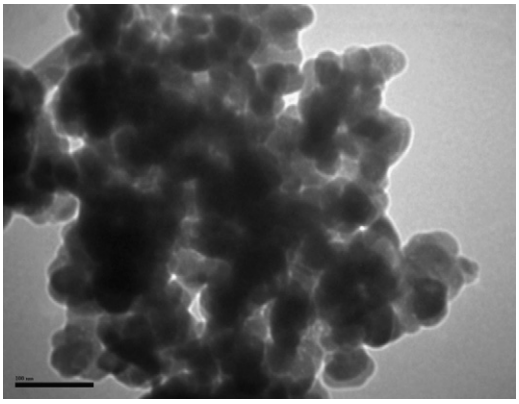

Fig. 8. TEM image of calcined HA-CP (0% Triton X-100).

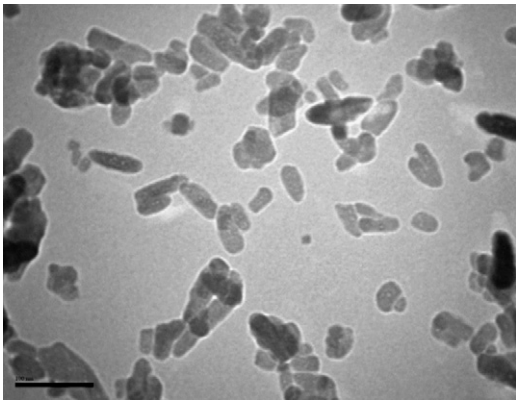

Fig. 9. TEM image of calcined HA-SA (4% Triton X-100).

agglomerated particles assuming approximately spherical morphology. The HA obtained via surfactant assisted route (HA-SA, 4% triton X-100) exists as discrete particles assuming rod like morphology. Thus triton X-100 plays a pivotal role in controlling the agglomeration of HA nanoparticles through physical interaction with primary particles prior to agglomeration. The particle size of HA nanorods synthesized in presence of Triton X-100 is calculated using UTHSCSA image tool software and found to be in the range between 35 and 72 nm in length and 16 and 26 nm in diameter. Thus TEM images confirm the formation of HA nano particles.

3.7. Probable mechanism for the effect of triton X-100 on particle size and surface area of synthesized HA

Fig. 10 depicts the structure of triton X-100. The stereochemical structure of the polyoxyethylene group of triton X-100 changes when dissolved in water due to solvation of polyoxyethylene groups. It has been an established fact that the oxygen atoms in the polyoxyethylene group of triton X-100 attracts the alkaline earth metal ions resulting in the formation of hydrophobic complex [26]. Mechanism of formation of nanoscale HA is represented schematically in Fig. 11. The square in Fig. 11 represents the hydrophobic group of triton X-100. Triton X-100 interacts with Ca^{2+} ions through an ion–dipole interaction of the polyoxyethylene

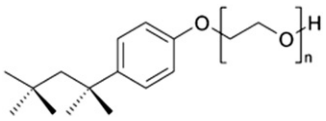

Fig. 10. Structure of Triton X-100.

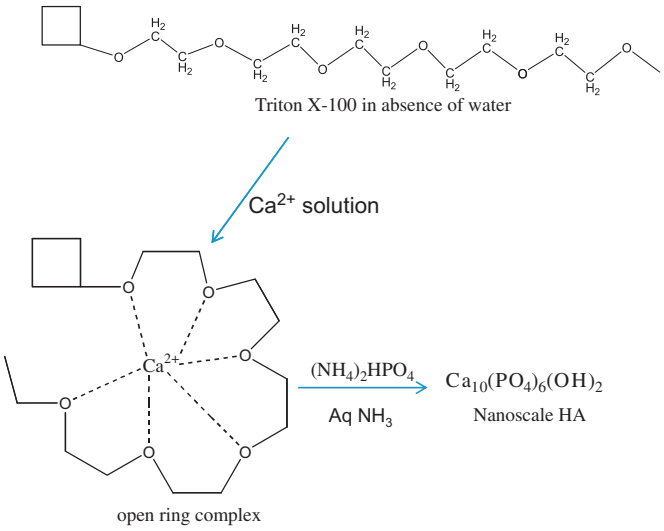

Fig. 11. Mechanism of formation of nanoscale HA.

group, thereby forming an hydrophobic open ring complex [26]. The transfer rate of Ca^{2+} ions to the growing crystals of HA is immensely reduced due to formation of the complex [23], thus leading to the formation of nanosized HA crystals under controlled conditions. In addition, triton X-100 gets adsorbed to certain planes of the formed HA crystals resulting in growth of HA particles in a preferential direction leading to the formation of nanorods. The fact that Ca^{2+} interacts with the polyoxyethylene group of triton X-100 in reducing the particle size has also been verified recently by Jingxian Zhang et al. [24] resulting in the preparation of rod like organized HA particles. Nevertheless, the details of measures undertaken for preventing the calcium ions from disrupting the micelle structure of triton X-100 [27] have not been presented by the authors. The present investigation used different preparation conditions than reported and focused on manipulating the role of surfactant as organic modifier rather than a template. The present work reports the formation of discrete and short nanorod like HA particles unlike the one reported in the literature [24]. Thus, this report serves as a complementing tool to further comprehend the dynamics of the interaction between metal ions and triton X-100 as surfactant from a different perspective under modified preparation conditions.

4. Conclusion

Hydroxyapatite particles having rod like morphology have been synthesized on nanoscale by a novel method using triton X-100 as organic modifier. As bone consists of rod like HA nano particles, it is expected that the HA prepared in the present investigation assuming rod form would be highly suitable as a biomaterial. The probable functional role presumed prior to the synthesis by using triton X-100 as organic modifier was to bring down the particle size of HA through physical interaction. The present investigation verifies the fact that indeed the surfactant reduces the particle size of HA through interaction. The strategy employed in the current investigation presents itself to be superior to using polyethyleneglycol as organic modifier as referred in the literature, (i) in imparting high crystallinity, (ii) in the formation of pure HA phase and (iii) in complete removal of surfactant. The present mechanism, proposed for the reduction of particle size, has potential in provoking one to think further in exploiting this method for understanding the role of such physical interactions in controlling texture and morphology. The effect of amount of surfactant on the stability of open ring complex formed with Ca^{2+} ions and the consequent effect in inhibiting the rate of crystal growth of HA and hence its particle size are potential problems to be resolved in future.

Acknowledgements

The authors would like to acknowledge the financial support by Department of Science and Technology, India, through the FIST programme to the Department of Chemistry, Madras Christian College, Chennai, India. They also acknowledge National Centre for Nanoscience and Nanotechnology (NCNSNT), University of Madras, Guindy campus, Chennai, India, for recording TEM images for their samples. Special thanks to Dr. S. Sriman Narayanan, Director of NCNSNT for providing the facility.

References

[1] M.Y. Shareef, P.F. Messer, R. Van Noort, Fabrication, characterization and fracture study of a machinable hydroxyapatite ceramic, Biomaterials 14 (1993) 69–75.
[2] J.M. Gomez-Vega, E. Saiz, A.P. Tomsia, G.W. Marshall, S.J. Marshall, Bioactive glass coatings with hydroxyapatite and Bioglass® particles on Ti-based implants 1. processing, Biomaterials 21 (2000) 105–111.
[3] John A.S. Bett, W. Keith Hall, The microcatalytic technique applied to a zero order reaction: the dehydration of 2-butanol over hydroxyapatite catalysts, Journal of Catalysis 10 (1968) 105–113.
[4] Said Sebti, Rachid Tahir, Rachid Nazih, Ahmed Saber, Said Boulaajaj, Hydroxyapatite as a new solid support for the Knoevenagel reaction in heterogeneous media without solvent, Applied Catalysis A 228 (2002) 155–159.
[5] Nabil Cheikhi, Mohamed Kacimi, Mohamed Rouimi, Mahfoud Ziyad, Leonarda F. Liotta, Giuseppe Pantaleo, Giulio Deganello, Direct synthesis of methyl isobutyl ketone in gas-phase reaction over palladium-loaded hydroxyapatite, Journal of Catalysis 232 (2005) 257–267.
[6] J. Sefton, M. Lambert, M. Wilson, H.N. Newman, Adsorption/desorption of amine fluorides to hydroxyapatite, Biomaterials 17 (1996) 37–46.
[7] Enrique D. Vega, Griselda E. Narda, Ferdinando H. Ferretti, Adsorption of citric acid from dilute aqueous solutions by hydroxyapatite, Journal of Colloid and Interface Science 268 (2003) 37–42.
[8] Gigliola Lusvardi, Gianluca Malavasi, Ledi Menabue, Monica Saladini, Removal of cadmium ion by means of synthetic hydroxyapatite, Waste Management 22 (2002) 853–857.

[9] Nilce C.C. da Rocha, Reinaldo C. de Campos, Alexandre M. Rossi, Elizabeth L. Moreira, Ademarlaudo do F. Barbosa, Gustavo T. Moure, Cadmium uptake by hydroxyapatite synthesized in different conditions and submitted to thermal treatment, Environmental Science and Technology 36 (2002) 1630–1635.
[10] Jie Fan, Jie Lei, Chengzhong Yu, Bo Tu, Dongyuan Zhao, Hard-templating synthesis of a novel rod-like nanoporous calcium phosphate bioceramics and their capacity as antibiotic carriers, Materials Chemistry and Physics 103 (2007) 489–493.
[11] Yaowalak Boonsongrit, Hiroya Abe, Kazuyoshi Sato, Makio Naito, Masahiro Yoshimura, Hideki Ichikawa, Yoshinobu Fukumori, Controlled release of bovine serum albumin from hydroxyapatite microspheres for protein delivery system, Materials Science and Engineering B 148 (2008) 162–165.
[12] Mansho Itokazu, Shinichi Kumazawa, Eiji Wada, Yang Wenyi, Sustained release of adriamycin from implanted hydroxyapatite blocks for the treatment of experimental osteogenic sarcoma in mice, Cancer Letters 107 (1996) 11–18.
[13] K.C.B. Yeong, J. Wang, S.C. Ng, Mechanochemical synthesis of nanocrystalline hydroxyapatite from CaO and $CaHPO_4$, Biomaterials 22 (2001) 2705–2712.
[14] M.H. Fathi, A. Hanifi, Evaluation and characterization of nanostructure hydroxyapatite powder prepared by simple sol–gel method, Materials Letters 61 (2007) 3978–3983.
[15] Y.X. Pang, X. Bao, Influence of temperature, ripening time and calcination on the morphology and crystallinity of hydroxyapatite nanoparticles, Journal of the European Ceramic Society 23 (2003) 1697–1704.
[16] Jingbing Liu, Xiaoyue Ye, Hao Wang, Mankang Zhu, Bo Wang, Hui Yan, The influence of pH and temperature on the morphology of hydroxyapatite synthesized by hydrothermal method, Ceramics International 29 (2003) 629–633.
[17] Guangsheng Guo, Yuxiu Sun, Zhihua Wang, Hongyou Guo, Preparation of hydroxyapatite nanoparticles by reverse microemulsion, Ceramics International 31 (2005) 869–872.
[18] Wantae Kim, Fumio Saito, Sonochemical synthesis of hydroxyapatite from H_3PO_4 solution with $Ca(OH)_2$, Ultrasonics Sonochemistry 8 (2001) 85–88.
[19] Jingbing Liu, Kunwei Li, Hao Wang, Mankang Zhu, Hui Yan, Rapid formation of hydroxyapatite nanostructures by microwave irradiation, Chemical Physics Letters 396 (2004) 429–432.
[20] Ying Jun Wang, Jing Di Chen, Kun Wei, Shu Hua Zhang, Xi Dong Wang, Surfactant-assisted synthesis of hydroxyapatite particles, Materials Letters 60 (2006) 3227–3231.
[21] R. Kumar, K.H. Prakash, P. Cheang, K.A. Khor, Temperature driven morphological changes of chemically precipitated hydroxyapatite nanoparticles, Langmuir 20 (2004) 5196–5200.
[22] Wei-Jen Shih, Moo-Chin Wang, Min-Hsiung Hon, Morphology and crystallinity of the nanosized hydroxyapatite synthesized by hydrolysis using cetyltrimethylammonium bromide (CTAB) as a surfactant, Journal of Crystal Growth 275 (2005) e2339–e2344.
[23] Chaofan Qiu, Xiufeng Xiao, Rongfang Liu, Biomimetic synthesis of spherical nano-hydroxyapatite in the presence of polyethylene glycol, Ceramics International 34 (2008) 1747–1751.
[24] Jingxian Zhang, Dongliang Jiang, Junling Zhang, Qingling Lin, Zhengren Huang, Synthesis of organized hydroxyapatite (HA) using triton X-100, Ceramics International 36 (2010) 2441–2447.
[25] Dae-Wook Kim, Seong-Geun Oh, Agglomeration behavior of chromia nanoparticles prepared by amorphous complex method using chelating effect of citric acid, Materials Letters 59 (2005) 976–980.
[26] Yoshida Zenko, Sorin Kihara, The role of non-ionic polyoxyethylene ether surfactants on ion transfer across aqueous/organic solution interfaces studied by polarography with the electrolyte dropping electrode, Journal of Electroanalytical Chemistry 227 (1987) 171–181.
[27] Virender K. Sharma, Rajiv Bhat, Thermodynamic studies on the interaction of some ureas and salts with micellar triton X-100 in aqueous solution, Thermochimica Acta 160 (1990) 315–322.